Journal of Nanotechnology & Advanced Materials
An International Journal

http://dx.doi.org/10.18576/jnam/050102

Annealing Temperature Effect on Hydrothermally Prepared Indium Oxide Spherical Nano Particles

E. Nirmala[*], *I. Kartharinal Punithavathy, S. Johnson Jeyakumar and M. Jothibas*

PG & Research Department of Physics, TBML College, Porayar 609307, India

Received: 19 Jul. 2016, Revised: 22 Sep. 2016, Accepted: 25 Sep. 2016.
Published online: 1 Jan. 2017.

Abstract: Indium oxide (In_2O_3) nano spherical crystalline particles have been prepared by hydrothermal technique at 350 ^{0}C, 400 ^{0}C and 450 ^{0}C. The prepared powder was characterized by XRD, SEM, TEM, UV and FTIR spectroscopy. The XRD confirms the spherical indium oxide nano particles were at single crystal phase with BCC and Rhombohedral structures. SEM and TEM indicate the formed In_2O_3 nano particles are with diameter 12nm. These findings should be of importance at both optical and electronic devices as well as theoretical investigations of the concerned crystal structure.

Keywords: In_2O_3, spherical nano particles, band gap, X-ray technique, FTIR, SEM, TEM.

1 Introduction

A wide band gap and high transparency In_2O_3 nano spherical particles has attracted some research attention in the applications of solar cells [1], gas sensors [2], photocatalysts [3], nano electronic building block and nano sensors. There are several type of synthesis techniques for preparation of In_2O_3 nanoparticles such as sol–gel [4, 5, 6], chemical vapor deposition [7, 8], and hydrothermal [9-11]. Recent studies on un-doped and doped In_2O_3 have mainly concentrated on preparation of various nano-structural shapes and their properties. For practical applications, a significant interest has been shown in the field of zero-dimensional and one-dimensional semiconducting In_2O_3 such as nano spheres [12], nano rods [13], nanofibers, nanowires [14] and nanoparticles [15-16]. Among other established synthesis methods, simple and cost effective routes to synthesize nano crystalline In_2O_3 by utilization of cheap, nontoxic and environmentally benign precursors are still the key issues, as well as the ability to control particle size and shape. Amongst these methods hydrothermal process have been widely used due to their simplicity, lower cost, and ability to control the particle size and shape. This method has been successfully used here to synthesize In_2O_3 nanoparticles with particle sizes of 12 nm.

In this paper, we report preparation and study of the structural properties of indium oxide nano-particles by hydrothermal method. The structural and shape characterization of nano-particles (powders) has been performed by the X-ray diffraction (XRD), scanning and transmission electron microscopy (SEM and TEM), and electron diffraction analysis. The optical band gap and bonding of molecules of the prepared nano-particles has been determined by the UV– vis optical absorption and FTIR spectroscopy measurement.

2 Experimental Details

In the present study, nano In_2O_3 was prepared by hydrothermal method. The chemical reagent was obtained from commercial source in analytical reagent (AR) grade and used without any further purification. A certain amount of $In(NO_3)_3.H_2O$ and 1,4 butadinol and deionized water was stirred to make it dissolved. Ammonia was added drop by drop to the solution to achieve a milk white colloidal gel state. After formation of white colloidal gel, it was kept in a constant temperature bath at 60°C for 20h and then further slowly heated until a light brown solution appear. The solution was washed with deionized water and dried at 30°C. Final product was placed into muffle furnace of different temperature and calcined for 3h and a pale yellow In_2O_3 powder obtained.

The calcined powder was characterized by X-ray diffraction (XRD) system in the 2θ range of 20–80° with Cu-Kα radiations (λ~1.5418 Å) operated at voltage of 30 kV and current of 15mA. The morphology and elemental analysis of the sample was done using a scanning electron microscopy with an energy dispersive spectrometer (EDS) respectively; the

[*]Corresponding author e-mail: enirmala138@gmail.com

particle size and morphology of nanoparticles have been studied using transmission electron microscopy (TEM) with an accelerating voltage of 200kv. UV-Visible measurements of the sample were performed in the range of 200–1100 nm using Spectrophotometer. Fourier transform infrared (FT-IR) spectroscopic analysis was carried out, using FTIR spectrophotometer in order to find the bonding changes in In_2O_3 powders samples.

3 Results and Discussion

3.1 FTIR Analysis

It is well known that vibrational spectroscopy is a very useful technique for the determination of the crystal phase of In_2O_3. The FTIR spectrum of In_2O_3 nano powder synthesized at the optimized preparation conditions is shown in Fig.1. Three main intense peaks centered at 440, 557, and 602cm^{-1} were observed, which is characteristic of the cubic In_2O_3 phase. According to the previous results reported in the literature, the observed bands at 440 and 557 cm^{-1} are attributed to In–O stretching in cubic In_2O_3 whereas the bands at 602 and 827 cm^{-1} is the characteristic of In–O bending vibrations in In_2O_3 [17].

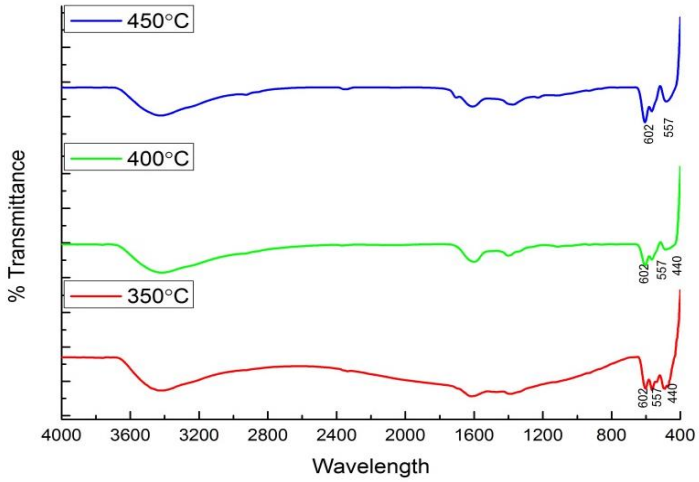

Fig.1 The FTIR spectra of 350,400,450^{0}C

Significantly, all the above bands have been reported in In_2O_3. The broad characteristic band at 557 cm^{-1} appears in In_2O_3 while a peak at 827 cm^{-1} corresponds to the In_2O_3 phase. In general, all three In_2O_3 polymorphs have very similar vibrational structures. A minor variation in their frequencies or relative intensities occurs in different In_2O_3 distributions in the interstitial sites. They are sensitive to the oxygen vacancies and other defects. These results reveal that the phase formation is complete for the as-prepared In_2O_3 nano powder and there is no evidence for the presence of any organic intermediates in the sample. The observed bands at 1595, 1552 and 1388 $cm^{-}1$ are attributed to C=O, C-O or (C=C aromatic) and C-H (aromatic) respectively of residues benzylamine acetate. The band around 3400 $cm^{-}1$ is attributed to the absorptions of hydroxyls from absorbing water or alcohols, because of the difficulty of removing the water residue completely.

3.2 Structural Analysis

The structural properties of the layers were measured using X-ray diffractometry (XRD). Fig(2) shows the XRD spectra of as-prepared samples at room temperature and that of annealed at different temperatures, 350 ^{0}C, 400 ^{0}C and 450 ^{0}C in oxygen ambient. Carbo thermal reduction of In_2O_3 powder during thermal evaporation is confirmed from the XRD data for the as prepared powder where a sharp diffraction peak related to indium is seen. The XRD spectrum of the annealed sample shows an intense peak at 350^{0}C that corresponds to the (104),(006),(116) and (300) plane of mixed cubic and rhombohedral In_2O_3. The observed diffraction peaks of (222), (400) and (622) match well with the cubic structure of In_2O_3 (JCPDS File No.22-0336), confirming the origin of the grown structures from In_2O_3. However, the crystal structure does not alter with annealing temperatures 400^{0}C and 450^{0}C. The XRD analysis further reveals that the intensity of the (222) peak increase noticeably at the temperature of 350^{0}C and continue to rise with further increase of temperature, indicating the preferential growth of In_2O_3 nano spheres along the (222) orientation with high crystallinity (JCPDS File No.06-0416).

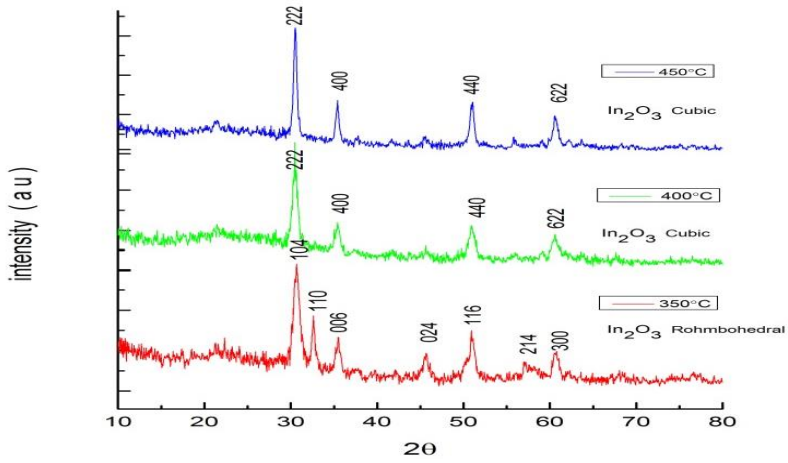

Fig.2. The XRD patterns of the In_2O_3 nano particles annealed at T= 350,400,450^{0}C

Table 1: XRD values and particle size in different temperature prepared by hydrothermal methods.

Temperature^{0}C	**350**	**400**	**450**
Hkl	104	222	222
	110	400	400
	006	440	440
	024	622	622
	116		
	214		
	300		
Particle size (nm)	**17.45**	**15.64**	**10.71**
Identification with (hkl) values	In_2O_3 -cubic & Rhombohedral	In_2O_3 -Cubic	In_2O_3 -Cubic

X-ray powder diffraction (XRD) patterns of as-prepared and annealed temperatures 400^{0}C and 450^{0}C In_2O_3 powders are shown in Fig.(2) match well with that of bulk cubic In_2O_3 reflections from (2 2 2), (4 0 0), (4 4 0) and (6 2 2) planes. XRD data further confirm the highly crystalline nature of the In_2O_3 nanoparticles. The XRD reflection peaks become broader as the particle size decrease, which is a general size dependent phenomenon within nanoparticles. The crystallite size was determined for the four major reflections of the XRD data by using the Debye-Scherer's equation and are listed in Table.1 From the structural information, it has been observed that the calculated values are equal or less than 20 nm, in agreement with the value determined from TEM images, indicating the single crystalline and spherical nature of individual nanoparticles.

$$D = k\lambda/\beta\cos\theta$$

3.3 Surface Morphology

The morphology of the In_2O_3 thin film was examined by scanning electron microscopy (SEM) operated at 20 kV. A typical SEM image for the film is shown in Fig.3 the approximately spherical In_2O_3 nanoparticles are easy to observe from this SEM image. The surface is covered with grains of uniform size and the grain size is found to be the maximum of about 20 nm. Transmission electron microscopy (TEM) SAED pattern observations show that indium oxide nanoparticles are spherical in shape with a narrow distribution of size as shown in Figs.4 & 5. The average size of nanoparticles is around 20 nm. TEM results give an average value over a population of particles, whereas the size distribution obtained by optical studies (e.g. UV-vis) can be unreliable due to contrast or agglomeration problems.

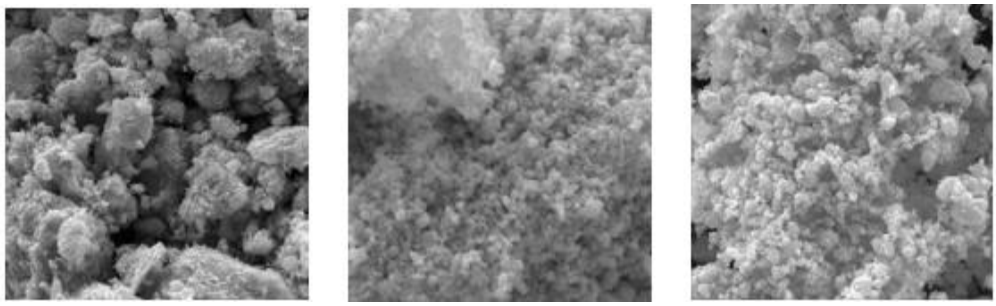

Fig.3. The SEM images of the In_2O_3 nano particles prepared by 350,400,450^{0}C.

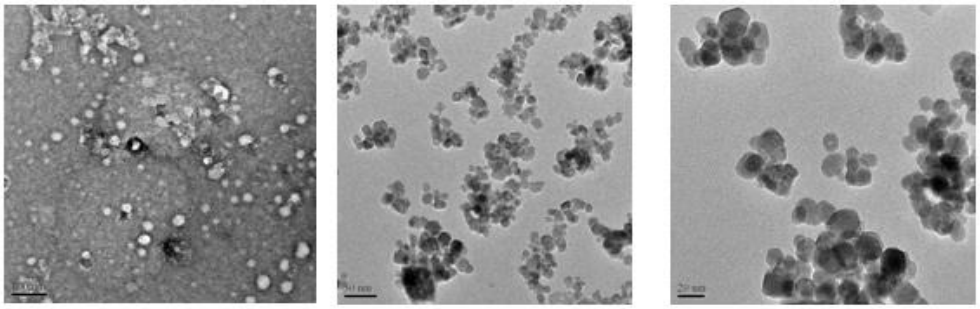

Fig.4. The TEM images of the In_2O_3 nano particles.

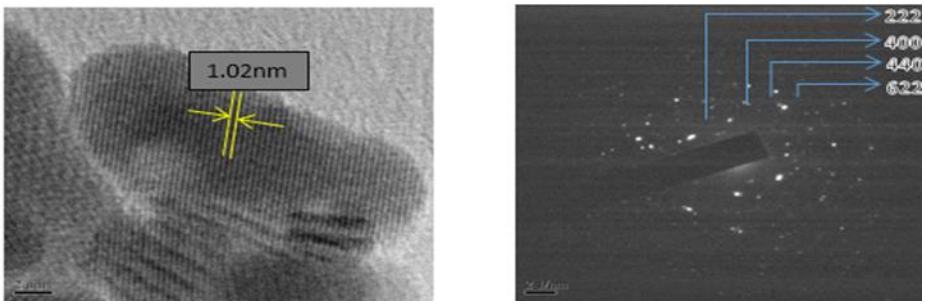

Fig.5. The TEM images and SAED pattern of In_2O_3 nano particles obtained.

3.4 UV Studies.

Figure (6) shows the optical transmittance range 200-1100 nm In_2O_3 powder. The optical transmittance of the powder is above 75% in the visible range. The optical absorption curve is located at about 200-400 nm. The absorption coefficients could be calculated from the transmission spectra in the UV region.

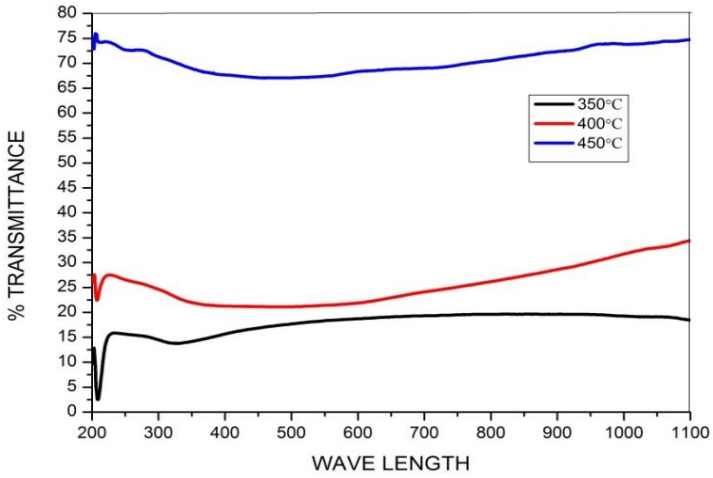

Fig.6. Transmission spectra of 350,400,450^{0}C

Optical constants of In_2O_3 powder such as the absorption coefficient have been calculated on the base of these absorbance experimental data. The optical band gap Eg of the powders were derived by plotting the relationship $(\alpha h\nu)^2$ vs photon energy, according to the well known Tauc procedure [18] assuming direct allowed electron transitions. Tauc plots of the investigated In_2O_3 powders are presented and the Eg values obtained by the extrapolation of the linear part are found to vary from 3.5 and 3.6 eV for different heat treated samples up to 450^{0}C (Fig 7). The effect of this powder on the transmission properties is also connected to the reduction in the free electrons scattering effect on the grain boundaries and the increase in carrier mobility. The absorption in the UV region is determined by the band gap electron transitions, and it has been established that the absorption edge shifts toward longer (red region) wavelength and most of the points fitted to a straight line graph. The values obtained for the direct band gaps are typical of a wide band gap semiconductor and are in good agreement with the reported data of In_2O_3 thin films.

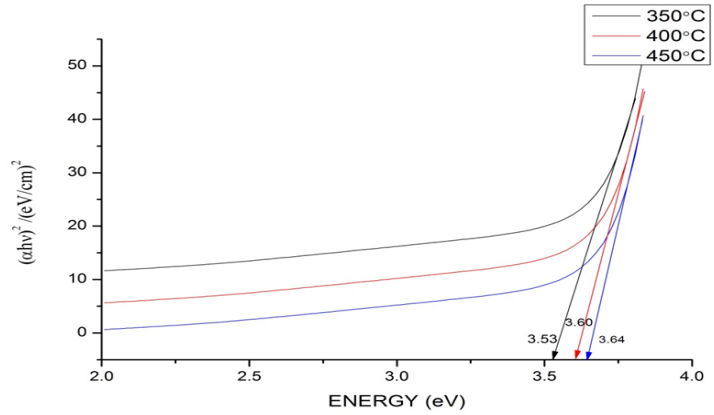

Fig.7. Tauc plot for In_2O_3 nano particles for determining the direct band gap.

4.Conclusion

Indium oxide nanoparticles, which are an important gas-sensing material, were prepared by a hydrothermal method. The particles calcined at 350-450^{0}C had a narrow size distribution and sphere-shaped particles. With an increase in annealing temperature in the range of 350-450^{0}C, nanoparticles grew considerably, and the size distribution became wide. The XRD

results show that pure cubic phase in 400^{0}C and 450^{0}C and mixed cubic and rhombohedral phase in 350^{0}C is obtained. The results of surface area analysis of In_2O_3 nano-particles show that in the hydrothermal method presence of particles with spherical shapes may lead to larger surface area. Therefore, the hydrothermal synthesis can be considered as a much suitable synthesis route for sensing applications.

References

[1] 1. Nakazawa T,Takamizawa K, Ito K. High efficiency indium oxide/cadmium telluride solar cells. Appl Phys Lett 1987;50:279–80.

[2] 2. Seetha M,Mangalaraj D.Nano-porous indium oxide transistor sensor for the detection of ethanol vapours at room temperature. Appl Phys A: Mater 2012;106:137–43.

[3] 3. Young S. C. and Young D. H., Controlled- Synthesis and Photocatalytic Properties of h-In2O3 and c-In2O3, Bull. Korean Chem. Soc., 2010; 3: 1769-1172.

[4] 4. J. Zhang, J. Hu, Z.Q. Zhu, H. Gong, and S.J. O'Shea, Quartz crystal microbalance coated with sol-gel-derived indium-tin oxide thin films as gas sensor for NO detection, Colloids Surf., A 236(1–3) (2004), pp. 23–30.

[5] 5. Hu SH, Liu TY, Huang HY, Liu DM. Langmuir 2008;24: 239–44.

[6] 6. Wang QY, Yu K, Xu F, Wu J, Xu Y, Zhu ZQ. Synthesis and field-emission properties of In2O3 nano structures. Mater Lett 2008; 62: 2710–3.

[7] 7. Hao YF, Meng GW, Ye CH, Zhang LD. Controlled synthesis of In2O3 octahedrons and nanowires. Cryst Growth Des 2005; 5: 1617–21.

[8] 8. V.A. Kuznetsov, Oxides of Titanium Sub group Metals, Crystallization Processes under Hydrothermal Conditions, Consultants Bureau, New York, 1973, pp. 43–55.

[9] 9. Min Guo, Peng Diao, et al., Hydrothermal preparation of high-oriented ZnO nanorod array films, Chemical Journal of Chinese Universities 25 (2004) 345–347.

[10] 10. Zhu MY, Diao GW. Journal of Physical Chemistry C 2011;115:18923–34.

[11] 11. K.Y. Kim, S.B. Park, Mater. Chem. Phys. 86 (2006) 210.

[12] 12. S.J. Limmer, K. Takahashi, G. Cao, Proc. SPIE 5224 (2003) 25.

[13] 13. C. Li, D. Zhang, X. Liu, S. Han,T.Tang, J. Han, C. Zhou, In2O3 nanowires as chemical sensors, Appl. Phys. Lett. 82 (2003) 1613–1625.

[14] 14. Y. Li, G. Xu, Y.L. Zhu, X.L. Ma, H.M. Cheng, Solid State Commun.142 (2007) 441.

[15] 15. R. Garkova, G. Volksch, C. Russel, J. Non-Cryst. Solids 352 (2006) 5265.

[16] 16. Souza E.C.C., Rey J.F.Q., Muccillo E.N.S., Synthesis and characterization of spherical narrow size distribution indium oxide nanoparticles, Appl. Surf. Sci. 2009; 255 Suppl. 6:3779–3783.

[17] 17. Rashed T. Rasheed , Sariya D. Al-Algawi , Sahar Z. Tariq, Preparation and Study of Indium Oxide Nanoparticles IJAP, Vol. 10, No. 4, October-December 2014, pp. 15-19

[18] 18. J. Tauc, F. Abeles, Optical Properties of Solids, North-Holland, Amsterdam, 1971.